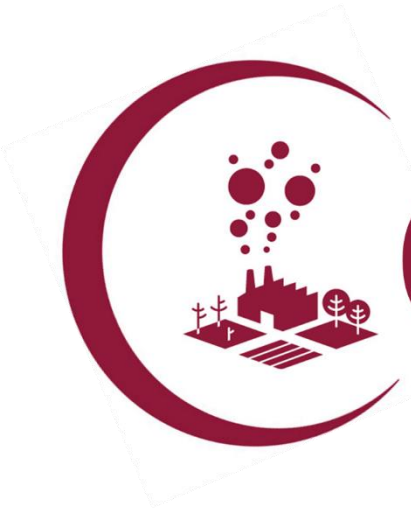

CONFESS

Consistent representation of temporal variations of boundary forcings in reanalyses and seasonal forecasts

Evaluation of the impact of variable land cover and vegetation on seasonal and near-term predictions

Constantin ARDILOUZE

Co-ordinated by ECMWF

CONFESS

Consistent representation of temporal variations of boundary forcings in reanalyses and seasonal forecasts

D3.3 Evaluation of the impact of variable land cover and vegetation on seasonal and near-term predictions, including recommendations for implementation

Author(s): Constantin Ardilouze (Météo France)
Magdalena Balmaseda (ECMWF)
Retish Senan (ECMWF)
Andrea Alessandri (CNR-ISAC)
Emanuele di Carlo (CNR-ISAC)

Dissemination Level: Public

Date: 25/01/2024
Version: 1.0
Contractual Delivery Date: 31/01/2024
Work Package/ Task: WP3/ T3.1 & T3.3
Document Owner: Meteo France
Contributors: ECMWF, CNR-ISAC
Status: Final

ECMWF METEO FRANCE CNRM BSC Barcelona Supercomputing Center Centro Nacional de Supercomputación ISAC

CONFESS

Consistent representation of temporal variations of boundary forcings in reanalyses and seasonal forecasts

Research and Innovation Action (RIA)
H2020- LC-SPACE-18-EO-2020 Copernicus evolution: Research activities in support of the evolution of the Copernicus services - Copernicus Climate Change Service (C3S

Project Coordinator: Dr Magdalena Alonso Balmaseda (ECMWF)
Project Start Date: 01/11/2020
Project Duration: 36 months

Published by the CONFESS Consortium

Contact:
ECMWF, Shinfield Park, Reading, RG2 9AX, United Kingdom
Magdalena.Balmaseda@ecmwf.int

The CONFESS project has received funding from the European Union's Horizon 2020 research and innovation programme under grant agreement No 101004156.

Contents

Figures

Tables

1 Executive Summary

This document outlines the progress and findings of the CONFESS project, focusing on integrating human-induced changes in land use and vegetation variability into seasonal forecast systems. Recent advancements in processing historical datasets have allowed for improved representation of temporal variability in seasonal forecasts. The primary objective is to evaluate the impact of these datasets and parameterizations on seasonal and decadal predictions and formulate recommendations for their integration into the next generation of the Copernicus Climate Change Service (C3S) systems. Notable findings include the limited impact of temporal variations in Land Use/Land Cover (LULC) on forecast skill but substantial influence on trend representation. Time-varying vegetation, both prognostic and prescribed, significantly impacts seasonal forecast skill, with diversity in the effects across systems and locations. Time-varying Leaf Area Index (LAI) compensates for LULC effects after 2000, balancing trends in certain regions but with exceptions. Additionally, it amplifies heat extremes in specific cases. Decadal predictions show improved skill, particularly in boreal winters. Recommendations include further research on temporal variations, understanding vegetation/atmospheric feedbacks, model improvements, and cautious operational implementation. While progress is evident, ongoing work is needed before full integration into operational forecasts is maximized.

2 Introduction

2.1 Background

Representing human-induced changes in land use and vegetation variability within physically based seasonal forecast systems has remained a blind spot of recent developments. The inability to model these processes prognostically has led to their exclusion from operational systems, resulting in a deficiency in monitoring and prediction. The lack of reliable temporal records further hinders the inclusion of temporal variations in the forecast systems included in Copernicus Climate Change Service (C3S) . Recent advances in reprocessing historical datasets for vegetation and land cover have offered an opportunity to improve the representation of temporal variability in seasonal forecasts. Since the beginning of the CONFESS project, state-of-the-art observational vegetation and land use datasets have been processed, evaluated and uptaken into land surface models. More specifically, substantial efforts have been made on improving a parameterization of the vegetation cover, processing and testing the disaggregation of vegetation observational datasets into model plant functional types, and assessing the validity of a prognostic vegetation scheme. The completion of this crucial initial stage has resulted in the identification of the most suitable vegetation and land-cover configurations for integration into fully coupled seasonal and decadal forecast systems.

2.2 Scope of this deliverable

2.2.1 Objectives of this deliverable

The objective of this document is to provide an evaluation of the impact of these datasets and parameterization on different aspects of seasonal and decadal predictions, and ultimately to formulate recommendations and pathways for their incorporation into the next generation of the C3S seasonal forecast systems to enhance their skill further.

2.2.2 Work performed in this deliverable

A number of seasonal and decadal reforecast experiments have been performed with 3 different prediction systems, using either fixed or time varying vegetation and land cover maps. The results are assessed through a range of evaluation criteria. The temperature prediction skill is measured across the full time period and with a focus on the two extreme summers of 2003 and 2010 over western Eurasia. The impact on temperature trends in summer and winter is also presented and discussed. Another section is dedicated to the potential predictability of vegetation anomalies based on a model using prognostic scheme for the leaf area index. The main conclusions of this evaluation are drawn in the final section, along with recommendations regarding the inclusion of time varying vegetation and land cover in forthcoming seasonal forecast systems.

2.2.3 Deviations and counter measures

None

3 DATA AND METHODS

3.1 Experiments and data

The numerical experiments evaluated in this deliverable consist of a set of 4-month seasonal hindcasts, with an ensemble size of 50 to 101 members, as well as 10-year decadal hindcasts, with 10 ensemble members. The hindcast have been initialized on May 1st and/or November 1st (See details in Table 1).

In all the "Perfect LAI" simulations, the prescribed LAI is derived from the CONFESS homogenized time series, described in Deliverable D1.1

Some of the experiments carried out by CNR (see details in Table 1) benefit from an improved effective vegetation cover parameterization in the HTESSEL land surface model, described in the CONFESS Deliverable D1.2. This development used satellite data on the fraction of green vegetation cover (FCover) from CGLS to formulate and integrate a spatially and temporally varying effective vegetation cover parameterization defined as an exponential function of LAI (Van Oorschot et al., 2023).

Partner	Exp ID	Hindcast period	initial date	lead-time (M months or N years for decadal)	Ensemble size	Spatial resol	LAI config	Land-Cover config	Other (Effective vegetation cover parameterization)
MF	MF-Eco	1993-2016	May 1st	4 months	50	Atm: 1.5° Oce: 1°	Climatology (Ecoclimap)	fixed	
MF	MF-Cntrl	1993-2016	May 1st Nov 1st	4 months	50	Atm: 1.5° Oce: 1°	Climatology (CONFESS)	fixed	
MF	MF-Perf	1993-2016	May 1st	4 months	50	Atm: 1.5° Oce: 1°	Perfect (Prescribed)	fixed	
MF	MF-Int	1993-2016	May 1st Nov 1st	4 months	50	Atm: 1.5° Oce: 1°	Interactive (prognostic)	fixed	
MF	MF-Luc	1993-2016	May 1st	4 months	50	Atm: 1.5° Oce: 1°	Interactive (prognostic)	Prescribed annually varying	
ECMWF	CONTROL	1993-2019	May 1st Nov 1st	4 months	101	Atm: 0.5° Oce:1°	Climatology (CONFESS)	fixed	

ECMWF	LAI+LULC	1993-2019	May 1st Nov 1st	4 months	101	Atm: 0.5° Oce:1°	Perfect (Prescribed)	Prescribed annually varying	
ECMWF	LULC	1993-2019	May 1st Nov 1st	4 months	101	Atm: 0.5° Oce:1°	Climatology (CONFESS)	Prescribed annually varying	
CNR-ISAC	DCP-SENS	1993-2019	Nov 1st	5 years	10	Atm: 0.5° Oce: 1°	Perfect (Prescribed)	Prescribed annually varying	Improved parameterization constrained through satellite C3S/CGLS FCOVER
CNR-ISAC	DCP-CTRL[1]	1993-2019	Nov 1st	5 years	10	Atm: 0.5° Oce: 1°	prescribed from historical simulation (r1) with dynamical vegetation on.	prescribed from historical simulation (r1) with dynamical vegetation on.	Effective vegetation cover not constrained with observations.

Table 1 list of numerical experiments

3.2 Verification data and metrics

The ERA5 reanalysis (Hersbach et al, 2020) has been used as a reference dataset for the hindcast evaluations.

The Anomaly Correlation Coefficient (ACC, Equation 1) serves as the main prediction skill metric in this document. The ACC measures the linear relationship between forecasted and observed anomalies, specifically focusing on the phase of variability. Importantly, it does not take into account the magnitudes of these anomalies.

$$ACC = \frac{\sum_{i=1}^{N}(f_i-\bar{f})(o_i-\bar{o})}{\sqrt{\sum_{i=1}^{N}(f_i-\bar{f})^2}\sqrt{\sum_{i=1}^{N}(o_i-\bar{o})^2}}) \quad \textit{(Equation 1)}$$

[1] The decadal control experiment consists of decadal hindcasts previously conducted at Barcelona Supercomputing Center (BSC) as their tier-1 (Component A1) contribution to the Decadal Climate Prediction Project (Bilbao et al., 2021).

4 Results

4.1 Impact of the vegetation and land-cover configuration on the prediction skill

4.1.1 Seasonal lead-times

Different JJA (Fig. 1) and DJF (Fig.2) hindcasts initialized on May 1st and Nov. 1st respectively, are evaluated by means of ACC difference patterns with respect to a reference hindcast. Overall, ACC differences delineate relatively small scale features detailed as follows.

Fig. 1 (a) and (b) show the impact of LULC and of its combination with LAI in the ECMWF forecast skill (correlation) for JJA. We see that LULC has limited impact on forecast kill. In comparison, LAI+LULC has stronger impact with marked improvements across subtropical North America, Sahel region of Africa, Central Asia, northern China and the Indian subcontinent. There is however, degradation in skill over the high latitudes including Eurasian region and Canada as well as the Amazon.

The bottom block of Fig. 1 shows the impact of different land aspects in Meteo-France. The choice of LAI climatology (CONFESS versus Ecoclimap, shown in Fig. 1c) visibly reduces the correlation skill over NorthWestern USA, Central Europe and Northern Siberia, while it shows some skill improvements over Alaska, tip of Greenland, South of US, Argentina/Chile and Western Australia. These areas are also visible with the prescribed time-varying vegetation (Fig. 1d), although with some modifications. For instance, the area of degraded skill over Europe moves to the North. The skill is also reduced over Europe with either prescribed or prognostic (Fig. 1e) vegetation. The skill degradation over Siberia is shared by the ECMWF results.

We note that in the MF model, the impact of LULC (measured as the difference in skill between experiments Mf-Luc minus MF-Int, fig. 1f) is stronger than in the ECMWF, with substantial, albeit localized, increase of ACC. The limited LULC sensitivity for ECMWF may be at least in part related to the vegetation discretization of HTESSEL that aggregates vegetation in only two tiles (high and low vegetation) for the computation of fluxes with the atmosphere in each grid point. In fact, differently from MF that allows coexistence of all plant functional types (PFTs), ECMWF allows only the dominant PFT for the low and the high vegetation tiles to characterise the respective biophysical parameters in each grid point (See Deliverable 1.2 for more details).

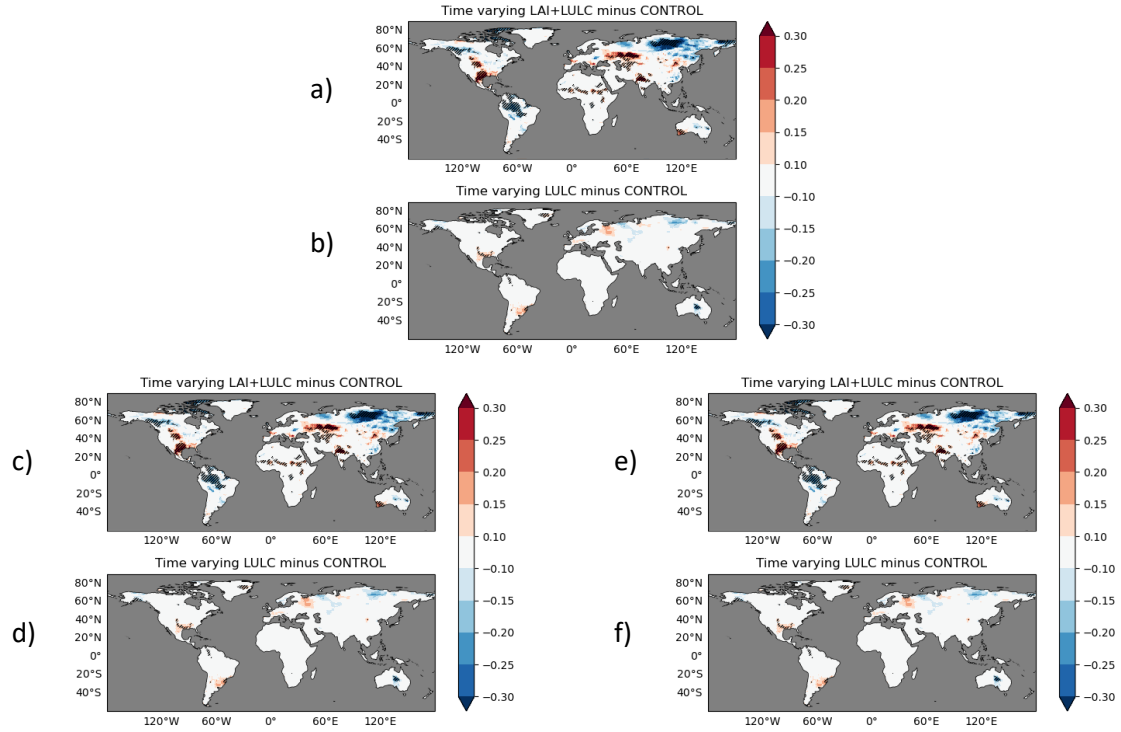

Figure 1: Anomaly Correlation Coefficient (ACC) for June-to-August seasonal mean 2m temperature in the ECMWF (top block, panels a,b) and Meteo-France (bottom block,panels c-f): (a) LAI+LULC and (b) LULC plotted as difference against the CONTROL experiment, in (c) MF-Cntrl (d) MF-Perf (e) MF-Int difference against MF-Eco and in (f) MF-Luc difference against MF-Int. Hashed areas are significant at 90% based on a Student's T-test.

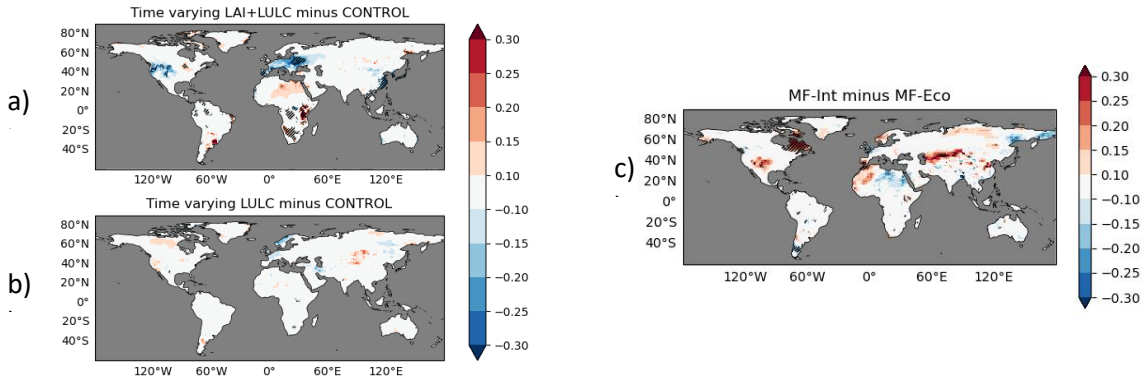

Figure 2: (a) and (b) Same as Fig. 1 (a) and Fig. 1 (b) but for December-to-February. (c) Mf-Int difference against MF-Eco for December-to-February

Fig. 2 shows the impact on skill for DJF. We see again that the LULC in the ECMWF system has little impact on skill (Fig. 2b). The time-varying LAI has a larger impact (Fig. 2a). It degrades the skill over Europe and Western USA, and shows some small and localized improvements over East Africa and South Brazil. In contrast, the prognostic LAI in the Meteo-France model (Fig. 2c) in DJF improves skill over Iberian Peninsula and Northern Africa, as well as large areas over the central US and along the Northern flank of the Himalayas.

In summary, we can conclude that time-varying LULC has little impact on the forecast skill of T2m, while time-varying LAI has visible impact on seasonal forecasts of T2m, affecting large areas. However, there is a large dispersion between models regarding the area of influence and the sign of the impact: in the ECMWF model the impact is largely negative, while in the Meteo-France model the impact is beneficial. Therefore, more research work is needed before using the new CONFESS datasets on operational reanalyses or seasonal forecasts. Another aspect to bear in mind is that at seasonal time scales the solution is likely to be dependent on the initial conditions, which in this work were produced without data assimilation.

4.1.2 Case studies: summers of 2003 and 2010

All the simulations show a relatively poor skill for t2m (not shown), which is not surprising given the weak summer temperature predictability over Europe (Patterson et al. 2022).

However, since the vegetation growth is highly sensitive to heat and drought stress, we wanted to assess the impact of the vegetation in the prediction of extreme summers such as 2003 for western Europe and 2010 for western Russia.

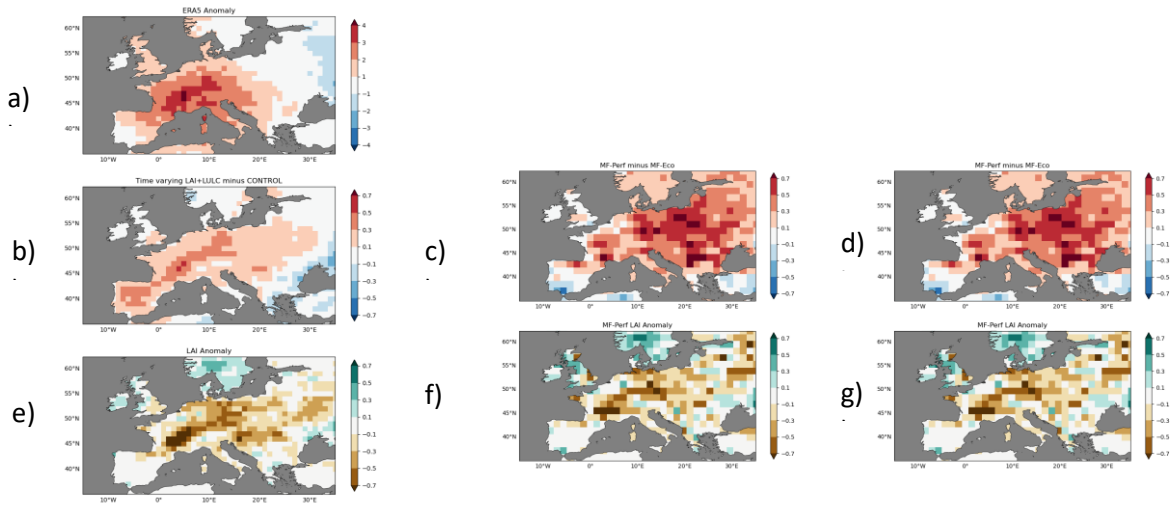

Figure 3. June-to-August 2003 seasonal mean 2m temperature over Europe: (a) ERA5 anomaly, (b) difference between LAI+LULC and CONTROL experiments, (c) MF-Perf and MF-Eco, (d) MF-Int and MF-Eco. (e) to (g) Leaf Area Index anomaly in LAI+LULC, MF-Perf and MF-Int, respectively.

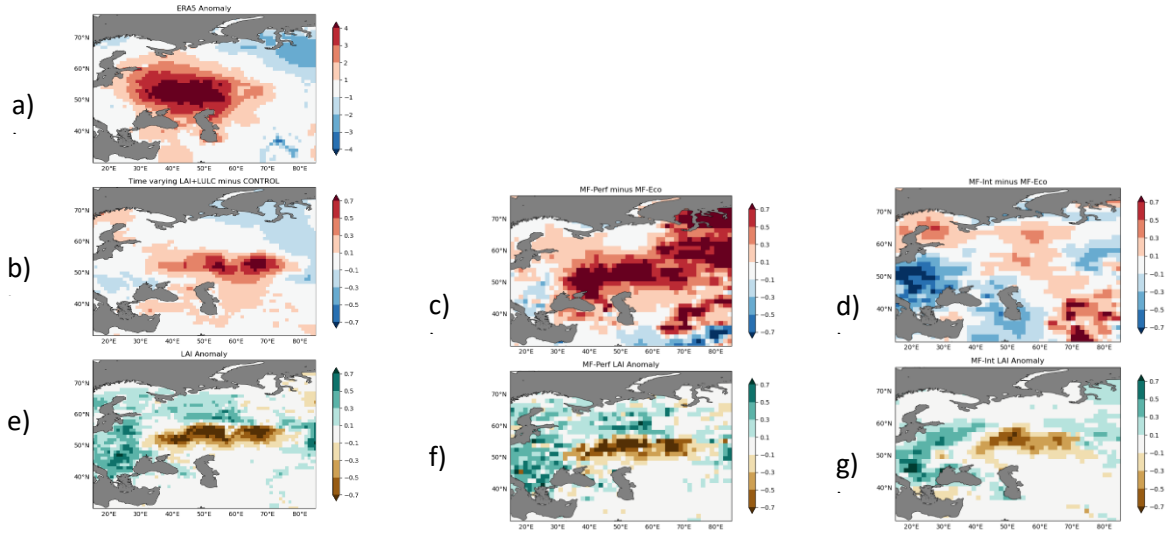

Figure 4. Same as Figure 3 but for 2010 over Russia

Time-varying vegetation improves the seasonal forecasts of heat extremes in both the ECMWF and MF models, when the LAI is prescribed (Fig. 3b,c and 4b,c). The region of maximum impact is collocated with those with negative LAI anomalies during both the European heat wave in 2003 (Fig. 3a) and the Russian heatwave in 2010 (Fig. 4a), although the temperature anomalies tend to have an excessive spatial spread in the Météo France model with prescribed time varying vegetation.

MF-Int succeeds in forecasting negative LAI anomalies in June-July-August for both case studies (Fig. 3g and 4g), with a slightly too strong amplitude in 2003 and too reduced in 2010. However, in 2003, the negative LAI anomaly pattern is located too far to the east. This could be one of the reasons why the temperature forecast fails in this experiment . In the 2010 case, despite an overall successful LAI forecast, the predicted temperature anomaly is not substantially better. For both case studies, we hypothesize that in the simulation using a prognostic vegetation scheme, the LAI suffer from initial conditions and time evolution different from observation, which might result in inadequate land-atmosphere feedbacks, and ultimately a loss of temperature forecast skill. Verifying this assertion would require further investigation.

4.1.3 Decadal lead-times

4.1.3.1 Improved representation of vegetation/land cover variability

The differences in the vegetation representation between the DCP-CTRL and DCP-SENS are evaluated by comparing the interannual variation of the annual-mean leaf area index (LAI) and the trends in annual-mean low and high vegetation covers. In the DCP-CTRL, the vegetation originates from an historical simulation of EC-Earth3 (EC-Earth3, historical, r1i1p1f1) that simulated vegetation dynamics (LPJ Guess; Smith et al., 2014), while in the DCP-SENS, the vegetation is prescribed using the new observational data from CONFESS (Deliverable D1.1) and also implementing the improved effective cover parameterization in CONFESS (Deliverable D1.2).

Figure 5 and Figure 6 show the interannual standard deviation for the high vegetation LAI and the low vegetation LAI, respectively. In figure 5, the high vegetation LAI reveals a discrepancy between the values simulated by LPJ Guess and the observed data that are prescribed in DCP-SENS. DCP-SENS exhibits the largest interannual variability in Euro-Asiatic boreal forests and North American subtropical humid and temperate forests (Fig. 5b). The North American boreal forest shows a relatively weaker interannual variability compared to other Northern hemisphere forests. Tropical forests in South America, Africa and Southeast Asia have low interannual variability, with typical values between 0.25 and 0.5.

The DCP-CTRL high vegetation LAI tends to underestimate the interannual standard deviation across various regions. The most significant differences from observations are found in the Northern Hemisphere, where the DCP-CTRL experiment struggles to capture the variability in North America and Eurasia (Figure 5a and 5c). DCP-CTRL also shows an unrealistically large interannual variability of the high vegetation over deserts (Fig. 5a). Despite this peculiar behaviour in the dynamical vegetation module, it does not impact the model, as the land cover is expected to prevent any effects resulting from this anomalous vegetation.

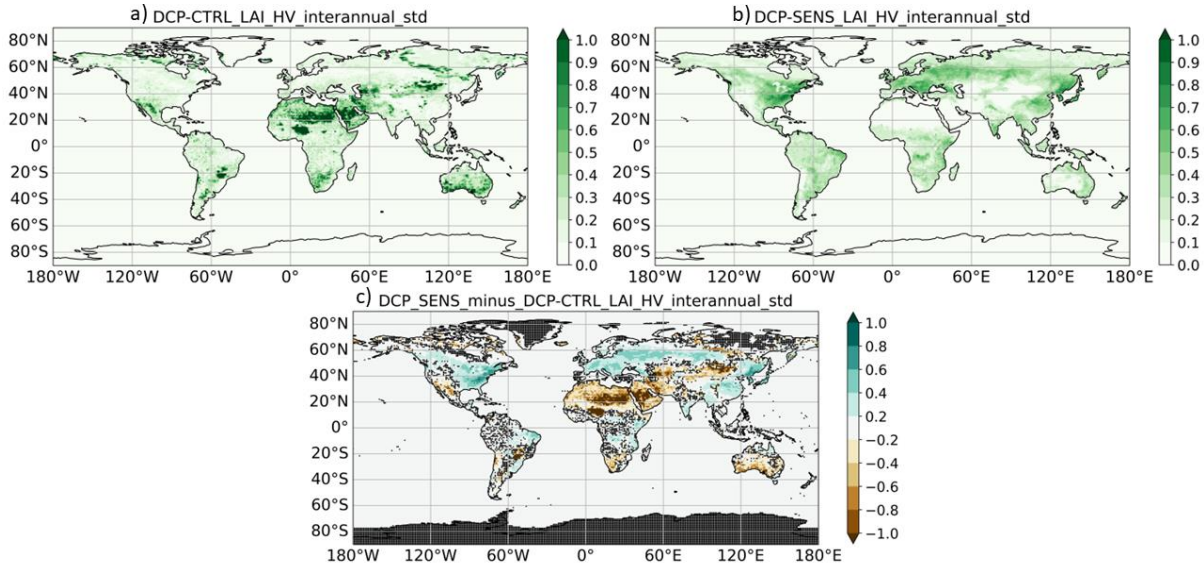

*Figure 5: Interannual standard deviation of high vegetation leaf area index (m^2/m^2). a) DCP-CTRL, b) DCP-SENS, c) DCP-SENS minus DCP-CTRL. Dots represent **not** statistically significant values, α=0.05.*

Figure 6 shows the interannual standard deviation for the low vegetation LAI. In contrast to the high vegetation case, the DCP-CTRL experiment (Figure 6a) exhibits a consistently higher interannual standard deviation of LAI compared to the observed data as prescribed in DCP-SENS. Differently from DPC-CTRL, the LAI variability of the low vegetation in DCP-SENS tends to be concentrated over regions where the low and high vegetation coexist. The largest difference between DCP-CTRL and DCP-SENS is evident in the Amazon forests, where DCP-CTRL exhibits an unrealistically high variability.

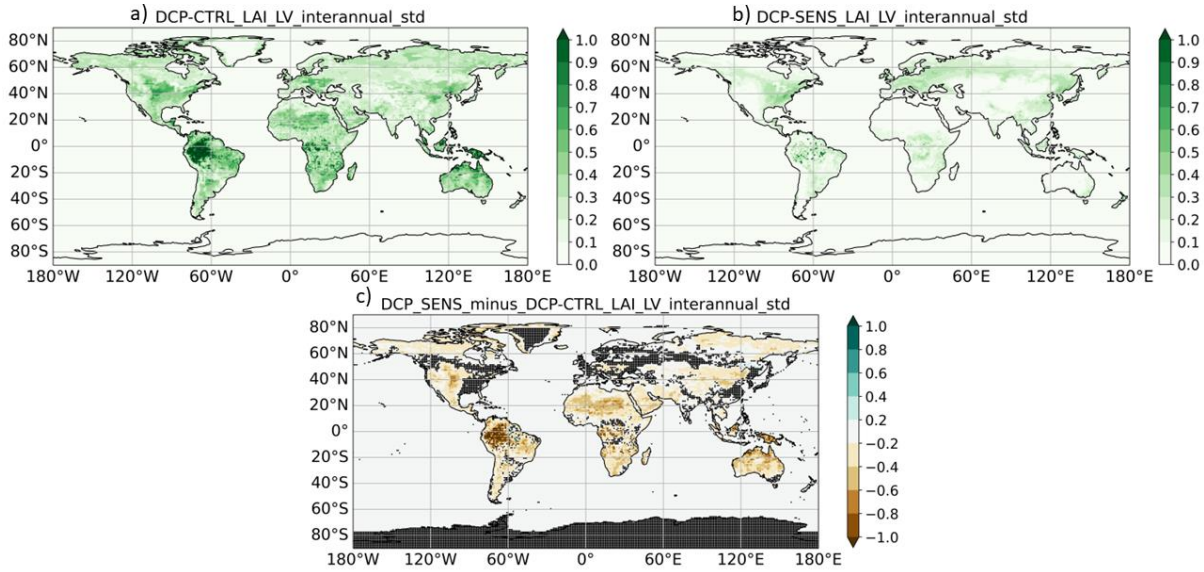

Figure 6: Same as Figure 5 but for the low vegetation leaf area index.

The trends of annual-mean effective vegetation cover are illustrated in Figures 7and 8 for high and low vegetation, respectively.

In figure 7a, the DCP-CTRL high vegetation effective cover trend is largely positive in Europe, the Euro-Asiatic boreal forests, and the northern limit of the North American boreal forest. Another considerable positive trend characterises the east-equatorial Amazon basin. On the other hand, negative trends characterise DCP-CTRL in the Southern Hemisphere, with larger values in Brazil and Argentina. Southeast Asia also exhibits a negative bias, while the signal in Africa is mixed.

Panel b displays the trend of the DCP-SENS experiment, which is positive in North America and Europe. A strong negative trend is observed in the Brazilian Amazon, confirming the deforestation process in that region.

The difference between the two experiments, as shown in panel c, indicates an excessive positive trend in the DCP-CTRL over Northern Hemisphere boreal and temperate forests. DCP-CTRL also overestimates vegetation trends compared to DCP-SENS over east-equatorial Amazon forest, while in the rest of South America the negative trends in DCP-CTRL are too large. In Africa, Southern Asia, Indonesia and Oceania the differences between DPC-CTRL and DPC-SENS tend to be mixed.

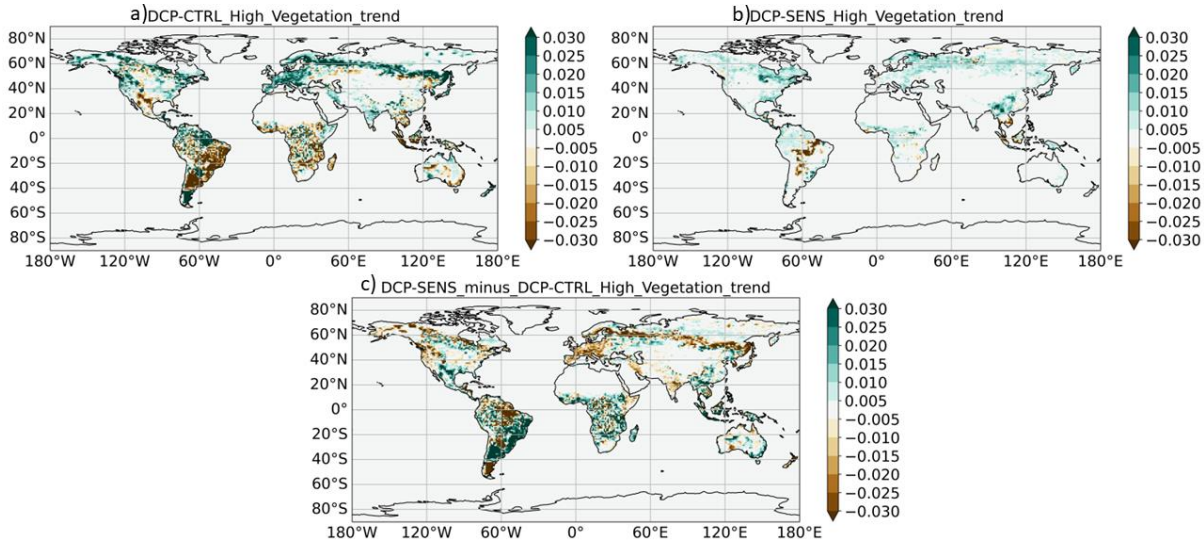

Figure 7: Effective high vegetation cover trend (%/10y). a) DCP-CTRL. b) DCP-VEG. c) DCP-SENS minus DCP-CTRL.

Figure 8 illustrates the trend in low vegetation (%/10y) displaying a considerable positive trend in low vegetation for both DCP-CTRL (panel a) and DCP-SENS (panel b) in large areas. DCP-CTRL (Fig 8a) shows a general positive trend across Euro-Asia, the Sahel, and North America. In Australia, there is a notable reduction in low vegetation in its eastern half, counterbalanced by an increase in the west. South America exhibits mixed trends with a significant increase in low vegetation over the Pampas region and a decrease in some parts of eastern Brazil and the extreme South of the continent. Conversely, the DCP-SENS experiment, and by design the observational data, shows a different pattern (Fig 8b and Fig 8c). While an overall positive trend in low vegetation is observed, this effect is localised to specific regions: Europe, Russia, United States and the Brazilian Amazon forests.

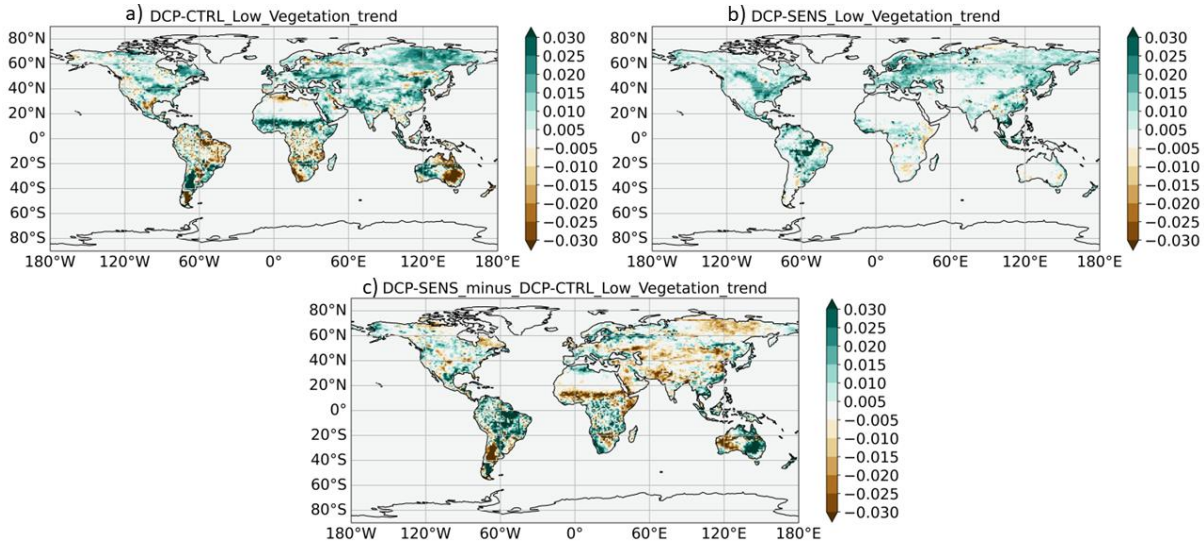

Figure 8: Same as Figure 7 but for the effective low vegetation cover.

4.1.3.2 Improved vegetation/land cover effects on Model bias

Figure 9 illustrates the global mean bias of the two-metre temperature as a function of the lead year. In panel a), the bias is calculated using all the grid points (land and sea). The DCP-SENS experiment (orange line) exhibits a consistently lower bias at every lead time, when compared to the DCP-CTRL experiment resulting in a global bias improvement of approximately 0.1K. As the simulation progresses, the model bias increases. For the DCP-CTRL experiment the two-metre temperature global average bias ranges from -0.6K at lead year 0 to -0.9K at lead year 4. Similarly, the bias for the DCP-SENS experiment shifts from -0.5K to -0.8K. To discern whether the bias reduction is attributed to land or ocean, Figure 9 panels b and c show the global bias calculated using land-only and sea-only grid points, respectively. The DCP-SENS experiment demonstrates a general improvement in bias compared to the DCP-CTRL experiment, with the most significant improvement occurring over land (Fig 9b), where the bias reduces by approximately 0.2K at each lead year. The differences over the ocean points are smaller, as expected since the differences between the two setups are in the land surface. Still, it is interesting to note that the properties of the vegetation over land in DCP-SENS appear to reduce slightly the biases over the ocean, as it is later shown in the bias maps (Fig. 10)

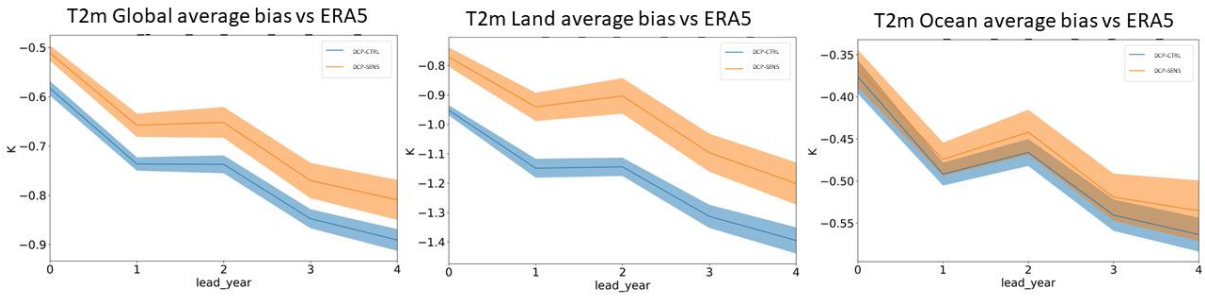

Figure 9: 2m temperature global average bias in function of the lead time. a) All the grid points, b) global average on land, and c) global average on ocean. The DCP-CTRL experiment is in blue and the DCP-SENS experiment is in orange. The line represents the ensemble mean values, while the shading is the ensemble spread.

Figure 10 compares the global maps of the bias in two-metre temperature. Panel a) displays the DCP-CTRL bias, panel b) illustrates the bias of DCP-SENS, and panel c) depicts the difference between DCP-SENS minus DCP-CTRL. Panels a) and b) demonstrate that the EC-Earth model generally exhibits a negative bias in two-metre temperature when compared with ERA5. In the Boreal hemisphere, larger cold bias values are observed over Sahara and boreal forests. Positive values are limited to three small regions: east of the Caspian Sea, and the east coasts of North America and Asia. The latter two regions are characterised by intense baroclinicity and are where the storm tracks originate. The southern hemisphere exhibits a different behaviour with the bias over the continents remaining negative, while it becomes mostly positive over the Southern Oceans, particularly at latitudes greater than 40S. The difference between the two experiments, as shown in Panel c), indicates an overall improvement in bias, particularly over Siberia, Europe, Greenland, and tropical forests (South America, Africa, and Southeast Asia). However, North American boreal forests and arid regions such as Sahara display an increase in the cold bias for DCP-SENS. The Northern Hemisphere Oceans also show a bias improvement over North Atlantic, Labrador Sea, Hudson Bay, North Pacific Ocean, and Bering Sea with a small (0.1K - 0.5K) but statistically significant reduction of the temperature bias. These improvements are localised in a latitudinal band between 40N and 80N.

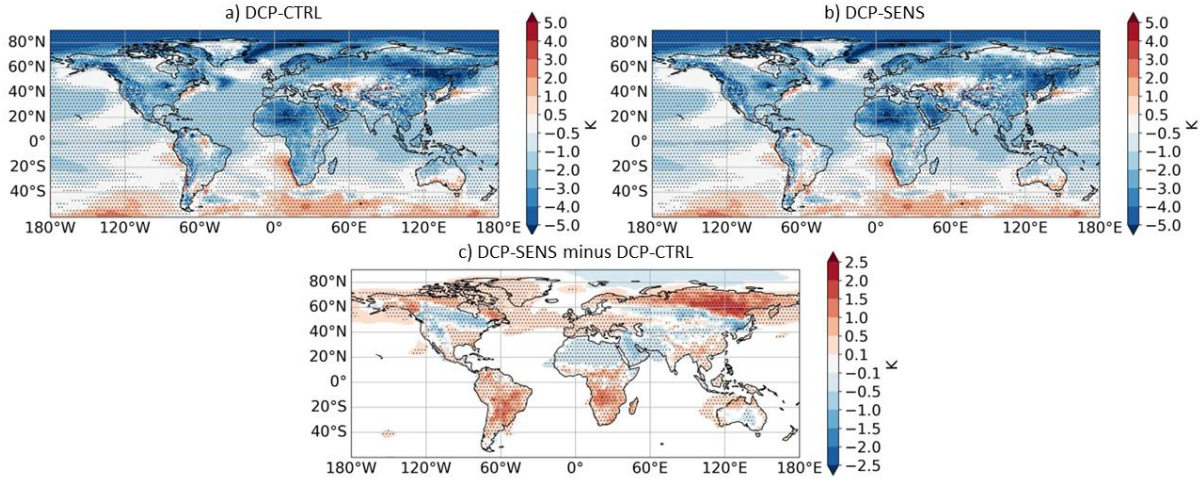

Figure 10: 2m temperature bias versus ERA5. a) DCP-CTRL bias. b) DCP-SENS bias. c) Bias difference, DCP-SENS minus DCP-CTRL. Dots represent statistically significant values, α=0.05.

4.1.3.3 Improved vegetation/land cover effects on Skill

Figure 11 shows the impact of the improved vegetation representation on the prediction skill, measured in terms of the Anomaly correlation coefficient (ACC), for annual-mean 2m Temperature at 3-year lead time, valid for the 4-5 year forecast period. The forecast start dates, in these figures, are limited from 1999 to 2019. The reduced sample of start dates is used to evaluate whether there is an effect due to the unrealistic LAI jump found for the tropical regions when moving from 1998 to 1999 (see deliverable D1.2). Figure 11a displays the ACC for DCP-CTRL, while Fig. 11b presents the ACC for DCP-SENS. The prediction skill of the model exhibits strong regional variation; some regions have high ACC values, while others have almost no skill. Over the continents, the prediction skill is limited but some regions display relatively good skill including the high latitudes (above 60N) in the boreal hemisphere (excluding Greenland and Canada), Central Europe, the Southwest of the United States, and North Africa. In contrast, the prediction skill of the model is low in Central Asia, North America (between 40N and 60N), and Greenland; these are regions where ACC values are near zero or negative. Focusing on the oceans, the Mediterranean, Indian Ocean, and Western Pacific Ocean (in the summer Intertropical Convergence Zone) are the basins with the highest ACC values. Conversely, the North Atlantic shows relatively low prediction skill.

When comparing the DCP-SENS and DCP-CTRL experiments (as shown in Figure 11, Panel c), it is shown that the ACC improvement is confined in a few regions with the most substantial signal concentrated in Central Asia boreal forest. Another strong signal is over the Bering Sea, and a third ACC improvement over the deciduous forests in the Southeast of the United States. The ACC improvement in Central Asia is in a region where the DCP-CTRL experiment has almost no skill and can be related to interannual variability in land cover introduced with the model's improved vegetation (figures 5 and 6). On the other hand, the skill improvement over the Bering Sea cannot be associated with changes in land cover but is most likely related to remote effects due to changes in nearby land masses.

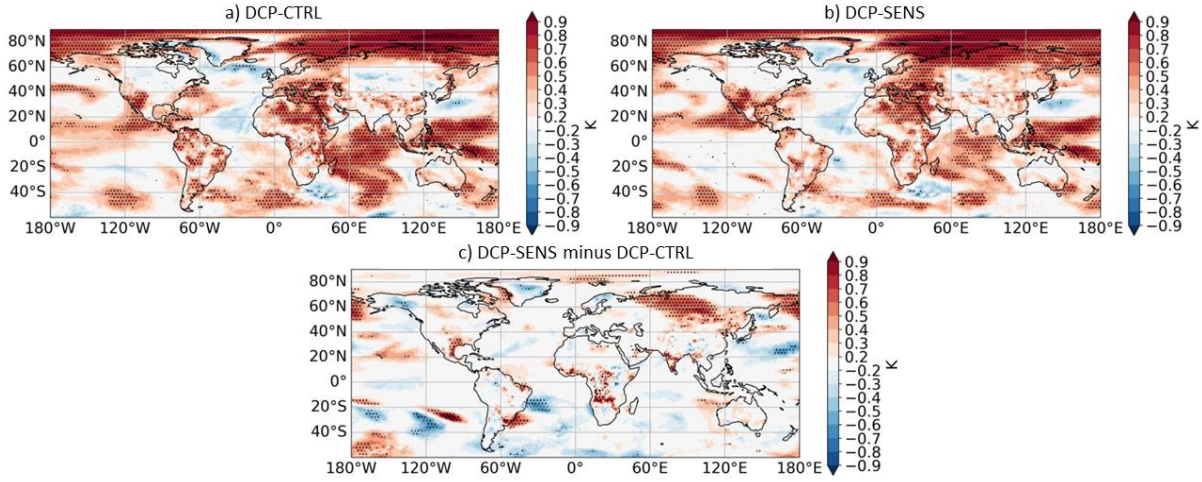

Figure 11: 2 m temperature annual mean ACC versus ERA5, at 3-year lead time, valid for the 4-5 year forecast period. a) DCP-CTRL ACC, b) DCP-SENS ACC, c) ACC difference, DCP-SENS minus DCP-CTRL. Dots represent statistically significant values, α=0.05.

Figure 12 shows the DCP-SENS minus DCP-CTRL ACC difference for the boreal winter season (December-January-February; DJF) at 3-year lead time, valid for the 4-5 year forecast period, for three different variables in polar stereographic projection: a) 2m temperature, b) mean sea level pressure (MSLP), and c) the zonal wind at 850 hPa. The polar stereographic projection is best suited to highlight the large-scale features of the Northern Hemisphere, i.e., where the improved vegetation has more significant effects. The difference in ACC for MSLP and U850 is visible over the region in Central Asia, where 2m temperature improves the most, but is also visible over a wide area to the West, including Europe and reaching the North Atlantic Ocean and Greenland. In North America, DCP-SENS shows a prediction skill improvement over Alaska, with a statistically significant reduction of the ACC values near the Hudson Bay.

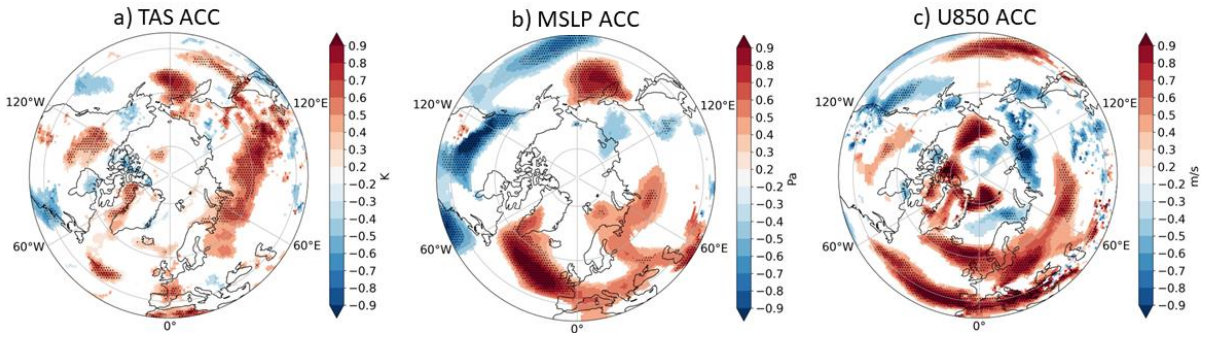

Figure 12: December-to-February season, ACC difference, DCP-SENS minus DCP-CTRL for 2 m temperature (a), mean sea level pressure (b) and zonal wind at 850 hPa (c). Dots represent statistically significant values, α=0.05.

4.2 Impact on the trends of screen-level temperature

4.2.1 Seasonal hindcasts

4.2.1.1 ECMWF

The impact of time varying vegetation in JJA in the ECMWF model is to dampen the observed warming trend (Fig. 13a) over most of the northern Hemisphere (Fig. 13b). It therefore worsens the trend errors (Fig. 13b) in most places including Europe and northern high latitudes. Land cover changes induce a significant reduction in errors over Central Eurasia (Fig 13d).

In boreal winter DJF, time varying vegetation leads to degradation in trends across most of the regions where changes are significant (South America, Greenland, sub-Saharan Africa, eastern Europe and Siberia) (Fig 14c).

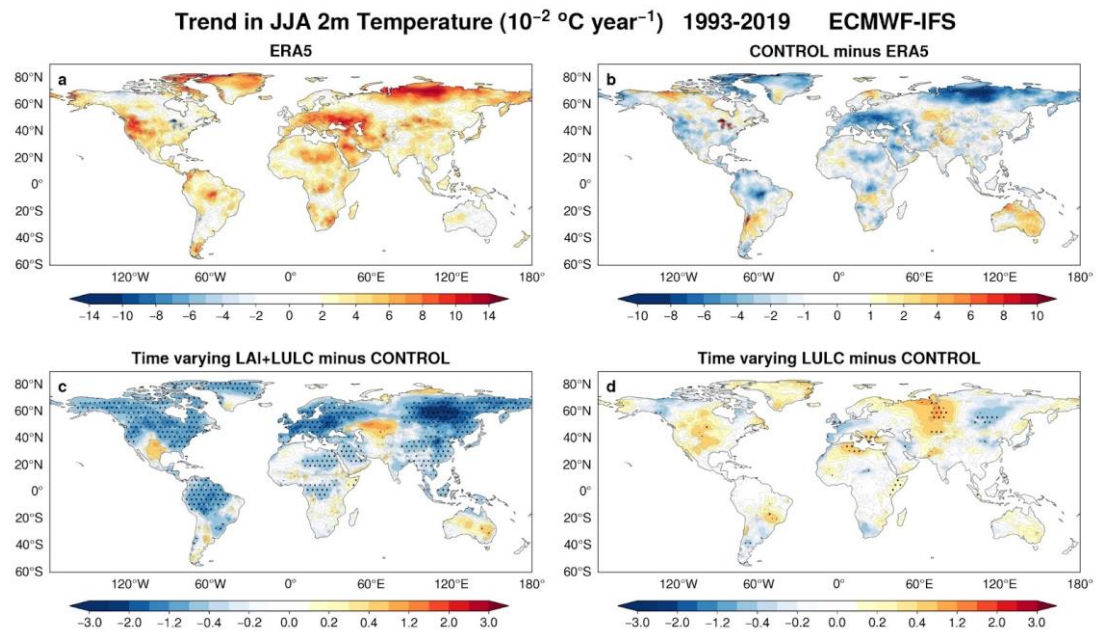

Figure 13: Trend in June-to-August seasonal mean 2m temperature during 1993-2019 in (a) ERA5 and differences against the CONTROL in the (c) LAI+LULC and (d) LULC experiments.

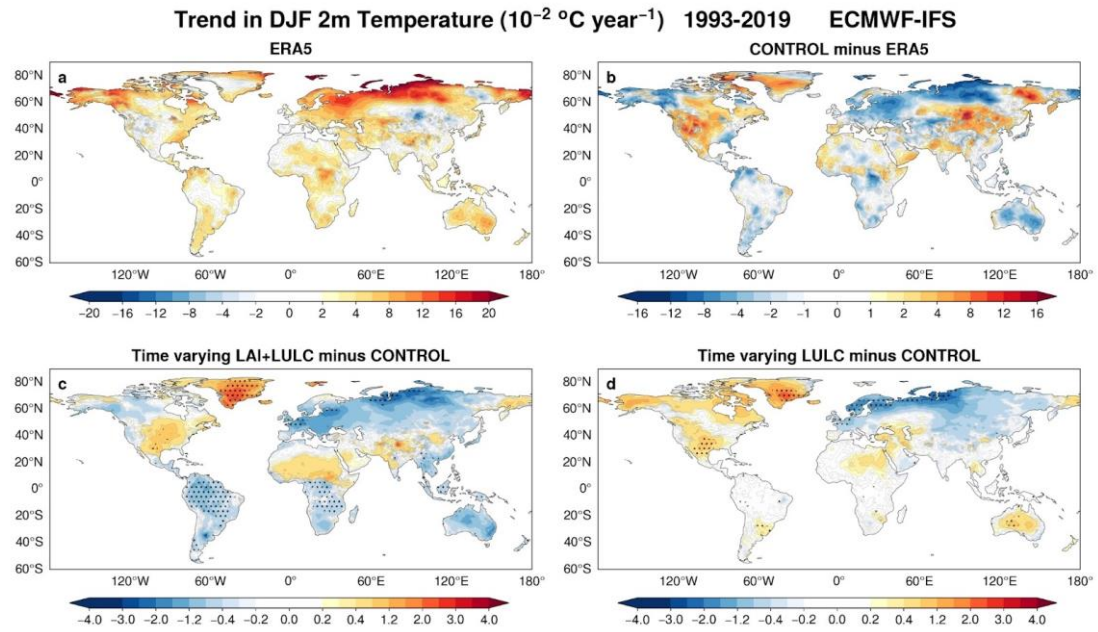

Figure 14: Same as Fig. 13 but for December-to-February.

4.2.1.2 Meteo France

The MF model captures relatively well the JJA linear trend of ERA5 (Fig 15a), and the difference patterns associated with the vegetation setup have a relatively low amplitude (Fig 15b). In more details, prognostic vegetation tends to reduce the positive trend errors over Canada, but to increase them over the Eastern USA. Overestimation of warming trends is reduced with prognostic vegetation in other areas, such as eastern Australia, North-West and southern Africa. However there are regions where prognostic vegetation increases the warming trends (western Europe, Central Siberian, Central Africa) and in these regions the trend errors get worse.

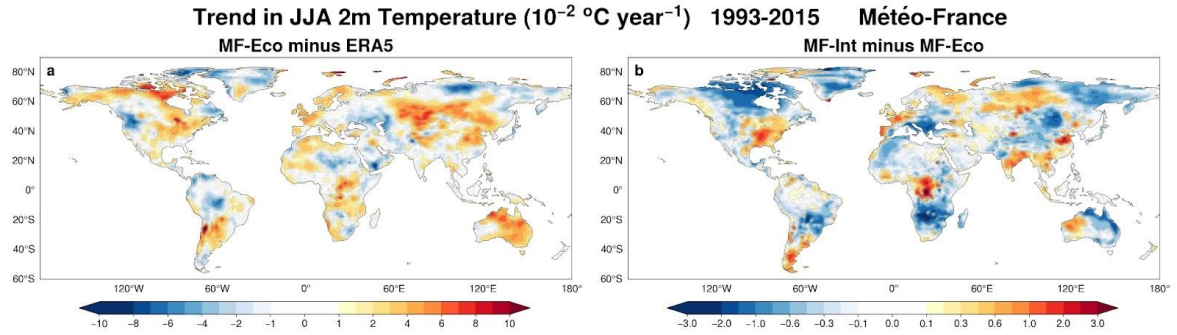

Figure 15: Trend in June-to-August seasonal mean 2m temperature during 1993-2015 as difference between (a) MF-Eco and ERA5 and (b) MF-Int and MF-Eco.

Figure 16 (top panels) compares the impact of prescribed time-varying vegetation, this time by comparing with MF-Ctrl (which uses the CONFESS climatology) rather than MF-Eco. The comparison is for seasonal forecasts of JJA initialized in May. Overall, the time-varying prescribed vegetation reduces the warming trend over most of the world. Notable exceptions are the surroundings of the Black and Caspian Sea (consistent with better representation of heat extremes in previous sections), Northern Africa (Mediterranean coast) and South Africa).

The prognostic vegetation (Fig 16c) does not show such an overall cooling impact w.r.t to MF-Cntrl. In fact, although the differences between Fig 15b and Fig 16c are sizable, they are only due to the reference LAI climatology (Ecoclimap and CONFESS respectively).

Finally, the impact of LULC in the Meteo-France model (Fig 16d) shows that time variations of this field also have a marked and large scale impact on T2m trends, and can add/damp the impact of prognostic vegetation.

In summary, just the choice of vegetation climatology or land use boundary conditions have substantial impact on the solution. These findings further illustrate the urgent need to pay attention to better representation of land processes in the models used for weather and climate prediction.

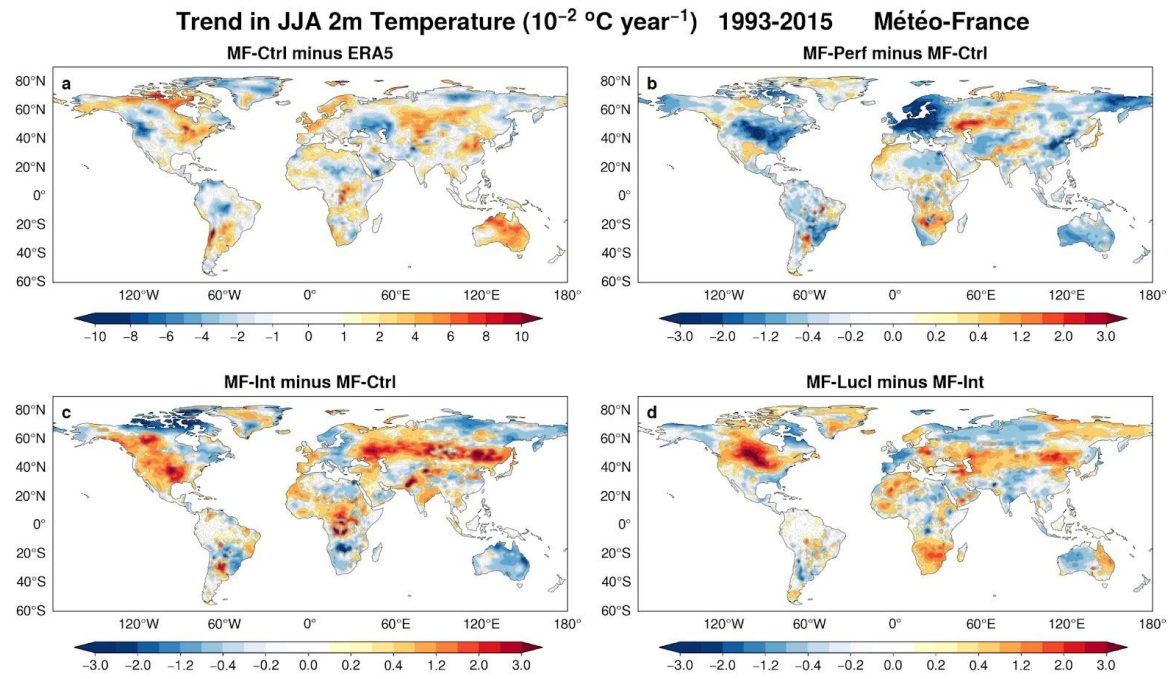

Figure 16: Same as MF but for differences (a) MF-Ctrl minus ERA5 (b) MF-Perf minus MF-Ctrl (c) MF-Int minus MF-Ctrl and (d) MF-Luc

As an illustration, Fig. 17 shows the LAI trend in MF-Perf (corresponding to the CONFESS LAI dataset) and in MF-Int for JJA 1993-2015. These trends are notably different, with MF-Perf exhibiting substantially higher trends over large areas of the globe, while MF-Int shows a mix of positive and negative trends with a weaker amplitude in general, with the exception of equatorial Africa. It is interesting to notice that many regions concerned by a negative LAI trend in MF-Int, (Central Africa, South east North America, eastern China) also show a positive anomaly of the temperature trend with respect to MF-Eco (trendless climatological LAI), and conversely (southern Africa, eastern Australia, eastern Siberia and northern Canada). The remarkable impact of LAI trend on temperature trend is

further confirmed by MF-Perf simulation, in which most the cooling hotspots correspond to a strongly positive LAI trend (northern Europe, North America, Amazon, China, eastern Siberia).

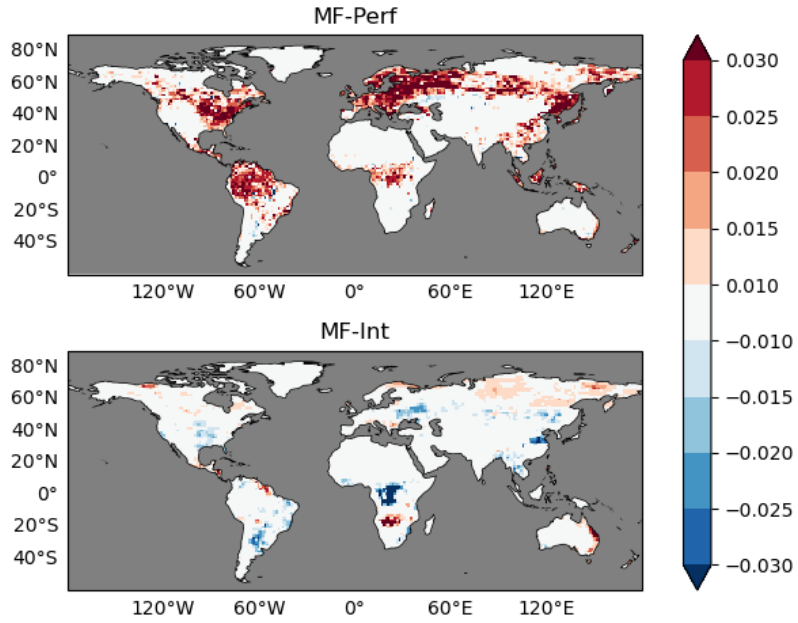

Figure 17: JJA 1993-2015 LAI trend in (top) MF-Perf and (bottom) MF-Int

Conversely to JJA, the model trend depicts a marked positive bias over central North America, as well as Siberia in DJF (Fig. 18a). The difference between interactive and climatological vegetation indicates an even stronger bias over central Canada and western Siberia (Fig 18b). However, in DJF prognostic vegetation reduces the negative trend errors over Western Canada and Alaska (~30%) and the positive trend errors over the USA (~10-20%). There is little impact over Europe.

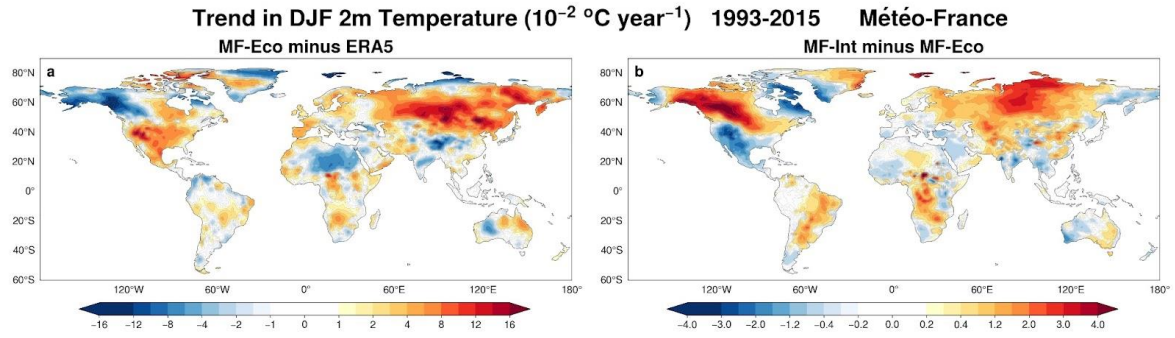

Figure 18: Same as Figure 15 but for December-to-February.

A misrepresentation of canopy-snow processes (Wang et al. 2016) and inaccurate snowpack initialization are likely involved in this discrepancy, and underlines the need to pursue investigation and increase the focus in this respect.

The impact on trends is generally larger scale than the impact on correlation skill. The impact is sizeable. To reiterate: vegetation has visible impact on trends, and grants further research, although it is not yet ready for operational implementation

4.2.2 Decadal hindcast trends

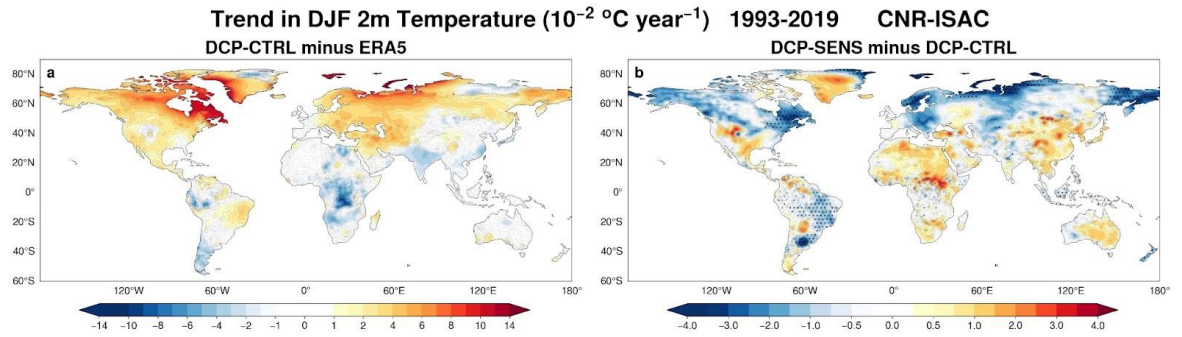

Figure 19: Trend in December-to-February, lead 3, two years mean, 2m temperature during 1993-2019 as difference between (a) DCP-CTRL and ERA5 and (b) DCP-SENS and DCP-CTRL. Stippling represents statistically significant values, α=0.05.

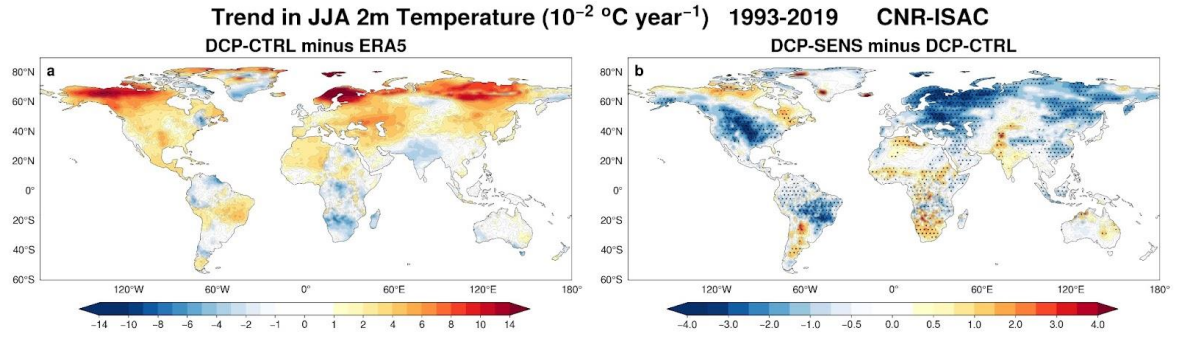

Figure 20: Trend in June-to-August, lead 3, two years mean, 2m temperature during 1993-2019 as difference between (a) DCP-CTRL and ERA5 and (b) DCP-SENS and DCP-CTRL. Stippling represents statistically significant values, α=0.05.

For the winter season (DJF, fig. 19), we find that the DCP-CTRL experiment tends to overestimate the temperature trends in the boreal hemisphere and Brazil. Conversely, the trend is underestimated in Africa, India and Argentina.

The introduction of realistic vegetation (DCP-SENS) improves the trend in several regions globally. The most significant improvements are observed in Quebec, Central Europe, Scandinavia, Alaska and the Far East of Russia. These improvements could be attributed to a better representation of the model albedo due to changes in snow cover and vegetation cover. However, Greenland exhibits a different behaviour and the trend degradetes. Outside of the boreal hemisphere, the DCP-SENS trend improves in Brazil but deteriorates in Africa and Australia.

For the summer season (JJA, fig. 20), similarly to DJF, the DCP-CTRL trend in JJA generally shows an overestimation. The regions with the largest trend bias are Alaska, Scandinavia and Siberia. North America, Central Europe/Middle East, China, Sahara and Brazil. Regions where the trend is underestimated include India and Southern Africa.

The comparison between DCP-SENS and DCP-CTRL shows a general improvement of the trends. Scandinavia, North America and Eurasia exhibit a significant improvement in the overestimated trend. Similarly, the temperature trend improves in Brazil, India and southern Africa.

The trend does not improve in a few regions, such as the Northern boundaries of the North American continent and the Sahel.

4.2.3 Impact of verification period on trends in ECMWF seasonal hindcasts

The temporal records of LAI presented a discontinuity in the tropics around 1999 (CONFESS Deliverable 1.1) which could contaminate the results presented above. In this section we repeat the diagnostics on trends for the period 2000-2019 with the ECMWF system. A shorter period means less significance of the trends, but also, since this period is more recent, we can expect stronger warming in ERA5.

Fig 21c and 22c show the impact of LAI and LULC on trends during this shorter period. The overall cooling impact of LAI during the longer record (Fig 13c/14c) is not so pronounced during 2000-2019, and it is hardly visible in South America or Africa. The absence of this cooling impact over these areas occurs in both JJA (Fig 21) and DJF (Fig 22). Therefore, we conclude that the strong cooling effect over these regions using the period 1993-2019 can be attributed to the discontinuity in the LAI record around 1999, which was larger in the tropical forests.

Fig 21d and 22d show that the impact of LULC is large and has different patterns for winter and summer. In JJA (Fig 21d), the time varying LULC impact manifests as a large scale structure over Eurasia, characterized by cooling over Western Europe and Eastern Asia, and a warming over Scandinavia Central Eurasia and around the Black Sea. There is also warming over North America. In DJF, the LULC (Fig 22d) produces an ever stronger large warming scale pattern over North America, but winter cooling over most of Eurasia.

The impact of time varying LAI seems to have a strong seasonal dependence, which mostly goes in the direction of damping the magnitude of the trends. Thus, in the summer hemisphere (JJA Fig 21c for NH and DJF, Fig 22c for SH), LAI induces a cooling trend in the high latitudes, which can dominate and reverse the signal induced by LULC. In the winter (DJF Fig 22 for NH and JJA, Fig 21 for SH), the time varying vegetation seems to also damp the cooling trends over Eurasia induced by the time-varying LULC. But there are notable exceptions to this damping effect: time-varying LAI enhances the warming trend in JJA over a vast area of Russia, and in DJF enhances the warming trends over Africa and Indian subcontinent.

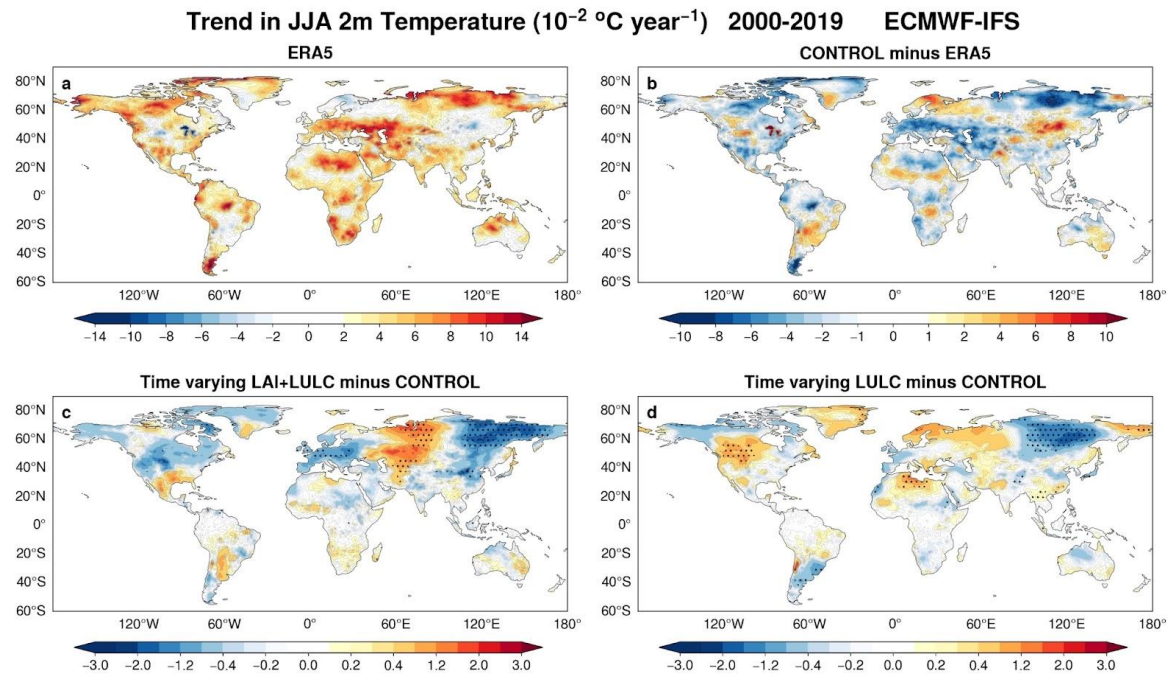

Figure 21: Same as Figure 13, but for the period 2000-2019.

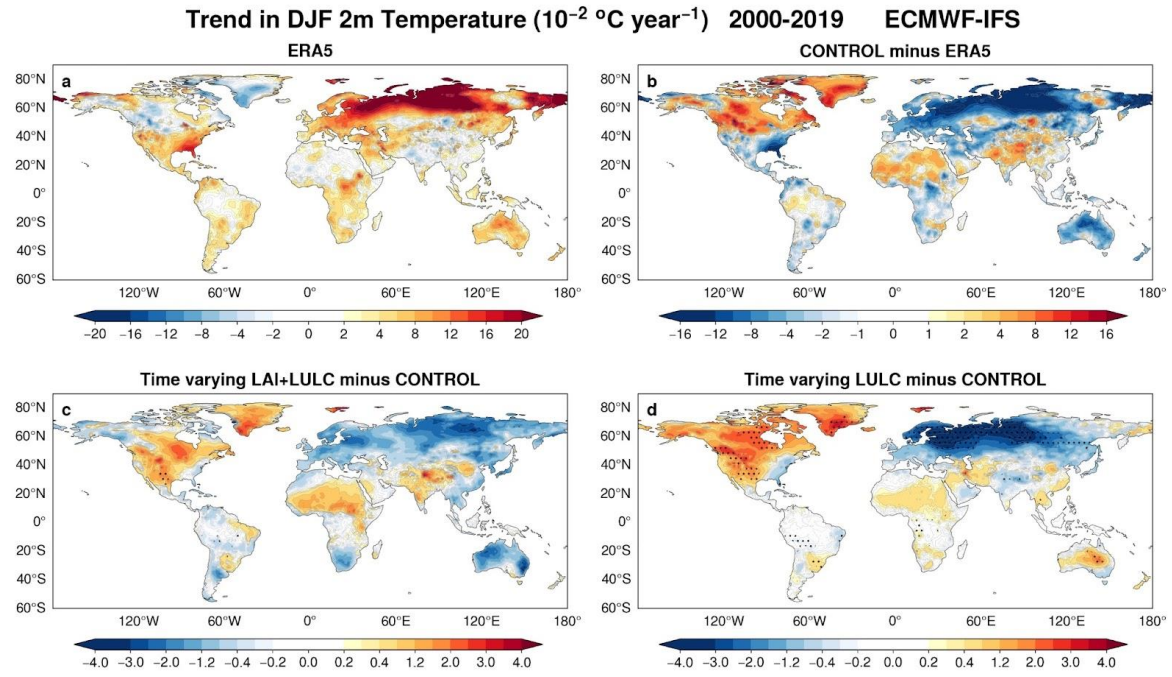

Figure 22: Same as Figure 14, but for the period 2000-2019.

4.3 LAI prediction: a proof of concept

Beyond the impact on climate trends and atmospheric seasonal predictability, the simulation with an interactive vegetation scheme allows us to assess the seasonal predictability of the LAI itself.

Predicting the LAI at the subseasonal and seasonal time horizon could help anticipate anomalies of gross primary production (GPP), and may foster novel climate services dedicated to agriculture and forest management.

Such a predictability assessment requires some benchmarking with a reference forecast system. Here, the reference is a persistence forecast, that consists in persisting the anomaly of LAI initial conditions across the seasonal cycle of a climatological LAI (eq. 2)

$$LAI^{y}_{persist}(t) = LAI^{y}_{Clim}(t) * \frac{LAI^{y}_{init}}{\overline{LAI_{init}}} \qquad \textit{(Equation 2)}$$

Where *y* is the considered hindcast year, and the overbar indicates the mean value across the full hindcast period.

The land component of MF-Int is initialised from the corresponding land offline simulation named *MF-ila* in Deliverable D1.2.

When the persistence forecast $LAI_{persist}$ is derived from actual LAI observation (namely the CONFESS homogeneized dataset, see deliverable D1.1), the LAI prediction skill exceeds MF-Int with very local exceptions (not shown). This relates to the fact that LAI initial anomalies may differ substantially between observation and MF-ila (cf. the analysis of the LAI bias if MF-ila, fig. 2 and 3 of Deliverable D1.2).

We have thus analysed the potential LAI predictability within a perfect model framework. In this case, the LAI time series derived from MF-ila is used as a synthetic truth. The ACC analysis (fig. 23d) reveals that the prognostic LAI beats the persistence across many regions at the seasonal lead time (boreal summer), with 2 noticeable exceptions over Northern Europe and Eastern US. Interestingly, the latter region matches very well a region dominated by C4 crop cover (See fig. 2 in Decharme et al., 2019). The sowing time of these crops, and maize in particular, revolves around late April or early May in the US. Consequently, the LAI anomaly taken on May 1st for C4-crop vegetation type may be little relevant to construct a persistence forecast. This hypothesis would deserve further investigation exceeding the scope of this project.

At a shorter lead time, the MF-Int is more skillful than the persistence across high latitudes only (fig. 23a and b). Over there, the vegetation is barely emerging from its winter dormancy on May 1st, which questions the relevance of persisting the LAI anomaly in these regions..

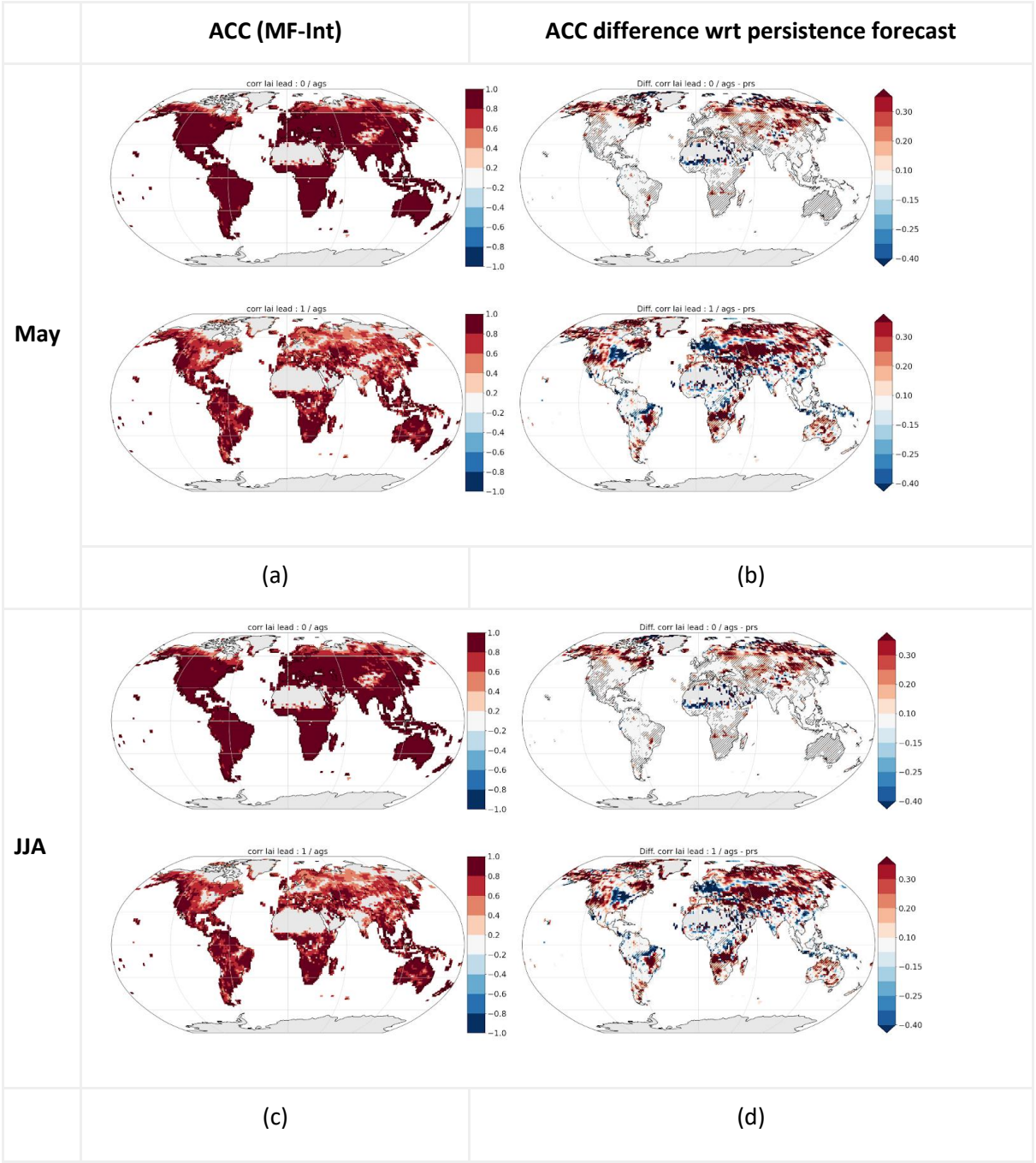

Figure 23: (a) May LAI anomaly correlation for MF-Int (b) Difference of anomaly correlation between MF-Int and a Persistent forecast. (c) and (d) like (a) and (b) for the June-July-August quarter

5 Conclusion and recommendations

The multi-model comparison anomaly correlation, linear trends and case studies in seasonal integrations conducted with time-varying LULC and LAI (either prescribed or prognostic), initialized in May and November, leads to the following conclusions:

- The temporal variations of LULC have little impact on forecast skill, but sizable impact (~10-20%) on the representation of trends, visible already at 3-months into the forecast, with strong seasonality.
- Time varying vegetation (both prognostic and prescribed) has a larger impact on seasonal forecast skill of T2m, but the impact is not robust across systems, varying largely on location and sign. There are also an indication that the choice of LAI climatology has a sizeable impact on forecast skill of T2m.
- There are indications that the discontinuity in the records of LAI around 1999 contaminate the representation of the linear trends in seasonal forecasts over the tropical areas.
- After 2000, the impact of time-varying LAI on seasonal forecasts of T2m trends is non negligible and commensurable with the impact of LULC. In several regions (especially high-low latitudes) it tends to compensate for the effect of time-varying LULC, reducing the cooling trends in the winter hemisphere and the warming trends in the summer hemisphere. But there are notable exceptions, such as the enhanced warming over large areas of Eurasia in JJA and over tropical Africa and Indian Subcontient.
- Time varying vegetation appears to increase the amplitude of heat extremes in specific cases, such as the heat waves of 2003 over France and 2010 over Russia.

The analysis of decadal integrations shows that the inclusion of an improved parameterization of the vegetation cover leads to considerably reduced temperature biases over continents. In terms of prediction skill, improvements are marginal when considering annual anomalies. However, for the boreal winter, the prediction skill is enhanced at the 3-year lead time, and this seems related to an improved atmospheric circulation. This suggests that the choice of vegetation boundary conditions in the models is crucial for both local land-atmosphere feedbacks and remote impacts associated with changes in circulation patterns.

Recommendations:

- More work is needed to understand the impact of temporal variations of LAI and LULC on seasonal forecasts, to reduce the uncertainty between models, and to evaluate the sensitivity to the initial conditions.
- Therefore, it is considered that the CONFESS developments are not ready yet for operational implementation in reanalyses and seasonal forecasts.

- There is a pressing need to quantify and verify the vegetation/atmospheric feedbacks in models at different time scales. This includes local thermodynamic effects and the possibility of vegetation and land use/cover to affect the atmospheric circulation.
- There is a strong need to improve the modelling of the time-varying properties in the models used for reanalysis and seamless forecasts from days to decades ahead.
- Improvements in the land/vegetation models are likely to feedback into the ability of data-assimilation methods to combine observational and model information, which will lead to better monitoring and initialization of seasonal forecasts. These improvements will in turn feedback in better abilities to verify forecasts and diagnose model errors

6 References

Decharme, B., Delire, C., Minvielle, M., Colin, J., Vergnes, J. P., Alias, A., ... & Voldoire, A. (2019). Recent changes in the ISBA-CTRIP land surface system for use in the CNRM-CM6 climate model and in global off-line hydrological applications. *Journal of Advances in Modeling Earth Systems*, *11*(5), 1207-1252.

Hersbach, H., Bell, B., Berrisford, P., Hirahara, S., Horányi, A., Muñoz-Sabater, J., et al. (2020). The ERA5 global reanalysis. Quarterly Journal of the Royal Meteorological Society, 146(730), 1999–2049. https://doi.org/10.1002/qj.3803

Patterson, M., Weisheimer, A., Befort, D. J., & O'Reilly, C. H. (2022). The strong role of external forcing in seasonal forecasts of European summer temperature. *Environmental Research Letters*, *17*(10), 104033.

Smith, B., Wårlind, D., Arneth, A., Hickler, T., Leadley, P., Siltberg, J., and Zaehle, S.: Implications of incorporating N cycling and N limitations on primary production in an individual-based dynamic vegetation model, Biogeosciences, 11, 2027–2054, https://doi.org/10.5194/bg-11-2027-2014, 2014.

van Oorschot, F., van der Ent, R. J., Hrachowitz, M., Di Carlo, E., Catalano, F., Boussetta, S., Balsamo, G., and Alessandri, A. (2023). Interannual land cover and vegetation variability based on remote sensing data in the HTESSEL land surface model: implementation and effects on simulated water dynamics. *Earth System Dynamics*, *14*(6), 1239-1259.

Wang, L., Cole, J. N., Bartlett, P., Verseghy, D., Derksen, C., Brown, R., & von Salzen, K. (2016). Investigating the spread in surface albedo for snow-covered forests in CMIP5 models. *Journal of Geophysical Research: Atmospheres*, *121*(3), 1104-1119.

Document History

Version	Author(s)	Date	Changes
V1.0	Constantin Ardilouze (Météo France)	24/01/2024	

Internal Review History

Internal Reviewers	Date	Comments
Jonathan Day (ECMWF)	22/01/2024	
Annalisa Cherchi (CNR-ISAC)	23/01/2024	

Estimated Effort Contribution per Partner

Partner	Effort
Météo France	14
ECMWF	
CNR-ISAC	
Total	**0**